July 2005

Mammalian Selenoprotein Thioredoxin-glutathione Reductase

Dan Su
University of Nebraska - Lincoln

Sergey V. Novoselov
University of Nebraska - Lincoln

Qi-An Sun
University of Nebraska - Lincoln

Mohamed E. Moustafa
NCI, National Institutes of Health, Bethesda, Maryland

You Zhou
University of Nebraska - Lincoln, yzhou2@unl.edu

See next page for additional authors

THE JOURNAL OF BIOLOGICAL CHEMISTRY Vol. 280, No. 28, Issue of July 15, pp. 26491–26498, 2005
Printed in U.S.A.

Mammalian Selenoprotein Thioredoxin-glutathione Reductase

ROLES IN DISULFIDE BOND FORMATION AND SPERM MATURATION*[S]

Received for publication, April 4, 2005, and in revised form, May 6, 2005
Published, JBC Papers in Press, May 18, 2005, DOI 10.1074/jbc.M503638200

Dan Su‡§, Sergey V. Novoselov‡§, Qi-An Sun‡§¶, Mohamed E. Moustafa‖, You Zhou, Richard Oko‡‡, Dolph L. Hatfield‖, and Vadim N. Gladyshev‡§§**

*From the ‡Department of Biochemistry and **Center for Biotechnology, University of Nebraska, Lincoln, Nebraska 68588, ‖NCI, National Institutes of Health, Bethesda, Maryland 20892, and the ‡‡Department of Anatomy and Cell Biology, Queen's University, Kingston, Ontario K7L 3N6, Canada*

Thioredoxin reductases (TRs) are important redox regulatory enzymes, which control the redox state of thioredoxins. Mammals have cytosolic and mitochondrial TRs, which contain an essential selenocysteine residue and reduce cytosolic and mitochondrial thioredoxins. In addition, thioredoxin/glutathione reductase (TGR) was identified, which is a fusion of an N-terminal glutaredoxin domain and the TR module. Here we show that TGR is expressed at low levels in various tissues but accumulates in testes after puberty. The protein is particularly abundant in elongating spermatids at the site of mitochondrial sheath formation but is absent in mature sperm. We found that TGR can catalyze isomerization of protein and interprotein disulfide bonds and localized this function to its thiol domain. TGR targets include proteins that form structural components of the sperm, including glutathione peroxidase GPx4/PHGPx. Together, TGR and GPx4 can serve as a novel disulfide bond formation system. Both enzymes contain a catalytic selenocysteine consistent with the role of selenium in male reproduction.

Thioredoxin reductases (TR(s))[1] are members of the pyridine nucleotide disulfide oxidoreductase family (1). In mammals, TRs are selenoproteins that contain a C-terminal penultimate selenocysteine (Sec) (2, 3), the 21st amino acid encoded by UGA. These enzymes are key components of the thioredoxin system, which is one of major redox systems in cells. They control the redox state of thioredoxin but were also implicated more broadly in redox regulation, cell growth, and other functions (4, 5). Two TRs, TR1 (also known as TrxR1 and Txnrd1) and TR3 (also known as TrxR2 and Txnrd2), have been characterized in detail and are components of cytosolic and mitochondrial thioredoxin systems, respectively. Both proteins have recently been shown to be essential for embryogenesis (6, 7).

Our search for new redox enzymes resulted in identification of thioredoxin (Trx)/glutathione (GSH) reductase (TGR) (8, 9), a new member of the TR family. Like TR1 (2–4), TGR contains a pyridine nucleotide disulfide oxidoreductase sequence and the Sec residue encoded by UGA (see Fig. 1) (8). However, compared with the 55-kDa subunit homodimeric TR1, TGR is composed of two 65-kDa subunits because it has an additional N-terminal glutaredoxin (Grx)-like domain (9). TGR was found to exhibit broad substrate specificity; it could act as TR, glutathione reductase, and Grx in *in vitro* assays (9). A Grx-containing form of TR1 was recently identified (10, 11); however, it displayed no activities characteristic of TGR (11).

Phospholipid hydroperoxide glutathione peroxidase (GPx4/PHGPx) is another selenium-containing protein. It reduces lipid hydroperoxides with GSH (12). This protein was found to also be a structural component of sperm (13). In elongating spermatids, the formation of the mitochondrial sheath in the sperm midpiece is thought to involve oxidative cross-links of structural proteins by GPx4, which itself becomes oxidatively cross-linked in mature sperm and changes its function from an enzyme to a structural protein of the mitochondrial capsule (13). In addition, structural features of the sperm flagella are stabilized by disulfide bonds, which appear to be regulated by testis-specific thioredoxins (14, 15). In the spermatid nucleus, chromatin condenses, and histones are replaced with protamines, which are stabilized by disulfide bonds that are thought to be generated by the nucleus-specific isoform of GPx4 (16). As a result of these and other processes, various nuclear and accessory structures in mature sperm become cross-linked by specific intra- and intermolecular disulfide bonds, which are preserved in the sperm until their reduction in fertilized eggs (17).

Despite the important roles that disulfide bond formation and isomerization play in sperm development, little is known about how these processes are accomplished or regulated and what cellular components are involved in redox-dependent sperm maturation. In the present work, a functional characterization and localization of TGR revealed its disulfide bond isomerization activity and its close functional relationship to GPx4. These data implicated TGR in the process of sperm maturation.

EXPERIMENTAL PROCEDURES

Isolation of Proteins—Mouse and rat TR1 and TGR were isolated from liver and testes using a three-step procedure (8, 18). The fragment encoding the Grx domain of mouse TGR was amplified with primers 5′-GAGATTCCATATGGCGTCGCCACCCGGCCGCCG-3′ and 5′-CG-

* This work was supported by Grant GM065204 from the National Institutes of Health (to V. N. G.). The costs of publication of this article were defrayed in part by the payment of page charges. This article must therefore be hereby marked "*advertisement*" in accordance with 18 U.S.C. Section 1734 solely to indicate this fact.

[S] The on-line version of this article (available at http://www.jbc.org) contains supplemental Fig. S1.

§ These authors contributed equally to this work.

¶ Present address: Dept. of Medicine, Duke University Medical Center, Durham, NC 27710.

§§ To whom correspondence should be addressed. Dept. of Biochemistry, University of Nebraska, Lincoln, NE 68588-0664. Tel.: 402-472-4948; Fax: 402-472-7842; E-mail: vgladyshev1@unl.edu.

[1] The abbreviations used are: TR, thioredoxin reductase; TGR, thioredoxin/glutathione reductase; GSH, glutathione; Grx, glutaredoxin; GPx4, glutathione peroxidase 4; Sec, selenocysteine; PBS, phosphate-buffered saline; DTT, dithiothreitol; tPA, tissue plasminogen activator.

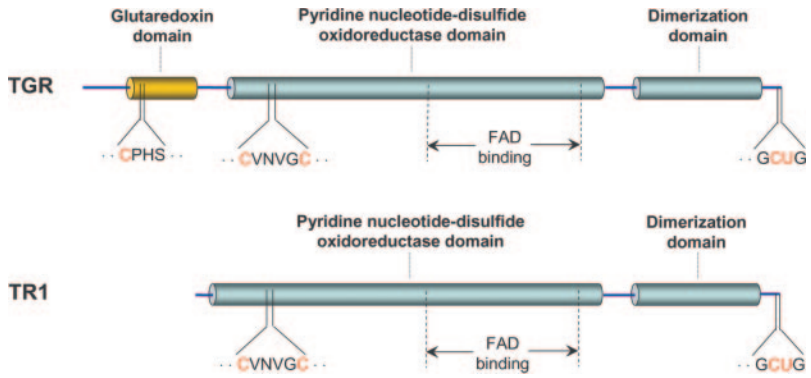

FIG. 1. **Domain organization of TGR and TR1.** Both enzymes contain a pyridine nucleotide-disulfide oxidoreductase domain, which includes binding sites for FAD and NADPH as well as the thiol/disulfide active site. TGR and TR1 also contain a dimerization (dimer interface) domain and a C-terminal GCUG (U is selenocysteine) active site. In addition, TGR has an N-terminal glutaredoxin domain. Conserved cysteine and selenocysteine residues that are involved in electron transfer are shown in *red*.

GAATTCTTAGTCATCTTGAAGGAGCTTCTGCA-3′ and cloned into pET28a (Novagen). The recombinant protein was expressed in BL21(DE3) and purified using nickel-nitrilotriacetic acid column (Qiagen) according to the manufacturer's manual.

TGR Expression Analyses—Approximately 0.2 g of various mouse tissues was sonicated in 5 volumes of 25 mM Tris-HCl, pH 7.5, containing 1 mM EDTA, 1 mM phenylmethylsulfonyl fluoride, 5 μg/ml aprotinin, 5 μg/ml leupeptin, and 5 μg/ml pepstatin A (buffer A). After centrifugation at 13,000 $\times$ *g* for 20 min at 4 °C, the supernatants were analyzed by immunoblot assay using antibodies specific for the C-terminal extension of TGR. Polyclonal antibodies that were raised against a full-length mouse TGR were also used.

Enrichment of Tissue TGR and TR1 on ADP-Sepharose—0.2–0.35 g of wild type mouse muscle, kidney, brain, prostate, lung, heart, liver, testes, and 1.0 ml of mouse blood was sonicated, and TGR was enriched on ADP-Sepharose (Amersham Biosciences) according to the manufacture's manual. The ADP-Sepharose-eluted fractions were analyzed by immunoblot assays with antibodies specific for TR1, TGR C-terminal peptide, and the full-length TGR protein.

Microscopy—Frozen sections (8 μm) were generated from wild type mouse testes and used for immunofluorescence labeling of TGR and GPx4. The sections were fixed in 4% paraformaldehyde in PBS, rinsed in PBS, and extracted with cold methanol at −20 °C for 5 min, followed by three washes in PBS and 1 h of blocking in 3% bovine serum albumin in PBS in the presence of 0.05% Tween 20 (PBST). The samples were then incubated for 2 h in PBST-containing 1% bovine serum albumin and primary antibodies against recombinant TGR and an internal peptide of mouse GPx4. The samples were washed three times in PBST, incubated in Cy5-conjugated donkey anti-rabbit secondary antibodies (1:100 dilution) (Jackson ImmunoResearch) in PBST containing 1% bovine serum albumin for 1 h, washed twice in PBST, and stained with 1 mM Sytox-green (Molecular Probes). After a 5-min rinse in PBS, they were mounted and examined on a Bio-Rad MRC1024ES confocal microscope using 488/647 nm excitation lasers and simultaneous display mode of the Bio-Rad LaserSharp imaging program.

Regulation of TGR Expression by Dietary Selenium—To obtain selenium-deficient mice, wild type weanling mice were maintained on a selenium-deficient Torula yeast-based diet (Harlan Teklad). To obtain selenium-sufficient mice, wild type mice were placed on a selenium-deficient diet that was supplemented with 0.4 ppm selenium as sodium selenite. After the indicated time on the diets, the mice were sacrificed, and tissues were extracted. Transgenic mice overexpressing i^6A^- mutant Sec tRNA (19) were maintained similarly on either selenium-deficient or selenium-sufficient diets. To label mice with ^{75}Se, 0.5 mCi of [^{75}Se]selenite was injected intraperitoneally, and mice were sacrificed 60 h later.

Isomerization of Interprotein Disulfide Bonds Involving GPx4 by TGR—Mouse or rat epididymal spermatozoa were solubilized with 0.1 M 2-mercaptoethanol and 6 M guanidine hydrochloride, followed by removal of low molecular weight compounds according to Ursini *et al.* (13). GSH only, TR1 and NADPH, or TGR and NADPH at the indicated concentrations were added to the 20-μg aliquots of solubilized sperm mixture, followed by incubation of the mixtures with 80 μM H_2O_2 for 15 min. Samples were then subjected to SDS-PAGE under reducing and non-reducing conditions followed by immunoblot assays using anti-GPx4 antibodies.

Formation and Isomerization of Disulfide Bonds in Ribonuclease A by GPx4 and TGR—Denatured reduced ribonuclease A was prepared as follows. Approximately 5 mg of native ribonuclease A was incubated in 1 ml of 100 mM Tris-HCl, pH 8.0, 6 M guanidine hydrochloride, 120 mM DTT, 0.2 mM EDTA, for 1.5 h at 37 °C. Low molecular weight compounds were removed using a PD-10 column that was pre-equilibrated with 0.1% acetic acid. RNase A and denatured reduced RNase A were quantified using absorbance coefficients $\epsilon_{275.5}$ = 9.8 $mM^{-1}\cdot cm^{-1}$ and $\epsilon_{275.5}$ = 9.3 $mM^{-1}\cdot cm^{-1}$, respectively.

The RNase A activity was determined by following the hydrolysis of cCMP as an increase in absorbance at 296 nm ($\Delta\epsilon_{296}$ = 0.19 $mM^{-1}\cdot cm^{-1}$). 5 mM cCMP was incubated with 1 μM denatured reduced RNase A and 2 μM H_2O_2-oxidized recombinant *Lycopersicon esculentum* GPx4 homolog, 2 μM oxidized glutathione, or 2 μM H_2O_2, which were used as oxidants in the assay. The mixtures were also supplied with 1 μM TGR, 1 μM TR1, or 7 μM reduced recombinant Grx domain of TGR (which provided isomerization/reduction function) in 0.5 ml of PBS, pH 7.4, for 45–60 min, as shown in Fig. 4. The differences in absorbance at 296 nm were used to calculate RNase A activity. Analogous experiments in which one or more of the components were absent were negative controls, and native RNase A was used as a positive control in the activity assays.

Isomerization of Disulfide Bonds by the Grx Domain of TGR in Escherichia coli Periplasm—The construct encoding the Grx domain of TGR targeted to periplasm (pPelTG) was cloned into a modified pET28 vector, in which the N-terminal His-tag sequence was removed and replaced with an N-terminal alkaline phosphatase periplasmic signal. The wild type strain and strains carrying pTrcStIItPA (expresses periplasmic tissue plasminogen activator (tPA)), pPelTG, or both plasmids were grown in LB medium at 30 °C until A_{600} reached 0.8, arabinose was added to 0.2%, 30 min later isopropyl 1-thio-β-D-galactopyranoside was added to 1 mM, and cells were grown for an additional 4 h. The periplasm was extracted according to the pET system manual (Novagen). Protein concentration was determined by the Bradford method (Bio-Rad).

Plasminogen activation assay was performed as described (20). Briefly, in a microtiter plate, 2.5 μg of a periplasmic protein fraction was added to wells containing 50 mM Tris-HCl, pH 7.4, 0.01% Tween 80, 0.04 mg/ml human glu-plasminogen, and 0.4 mM Spectrozyme PL (American Diagnostica), in a 260-μl final volume. The plate was incubated at 37 °C, and absorbance at 405 nm was read after 2 or 3 h. The activity was directly proportional to ΔA_{405} (absorbance after subtracting the background of a strain expressing an empty vector).

Identification of TGR Substrates—The recombinant TGR Grx domain was immobilized on CNBr-activated-Sepharose 4B (Amersham Biosciences) according to the manufacturer's protocol. Rat sperm was solubilized as described above, followed by the removal of denaturing and reducing agents by dialysis. The Grx resin was placed in a tube containing a sperm sample, rolling head to tail for 30 min at room temperature. The unbound proteins were removed, and the resin was washed 3 times with 0.1 M Tris-HCl, pH 7.4, 150 mM NaCl, 0.1% Triton X-100. The bound proteins were then eluted with 10 mM DTT, subjected to SDS-PAGE, and visualized by staining with Coomassie Blue. The protein bands were cut, and protein identities determined by tandem mass spectrometry sequencing at the University of Nebraska mass spectrometry facility.

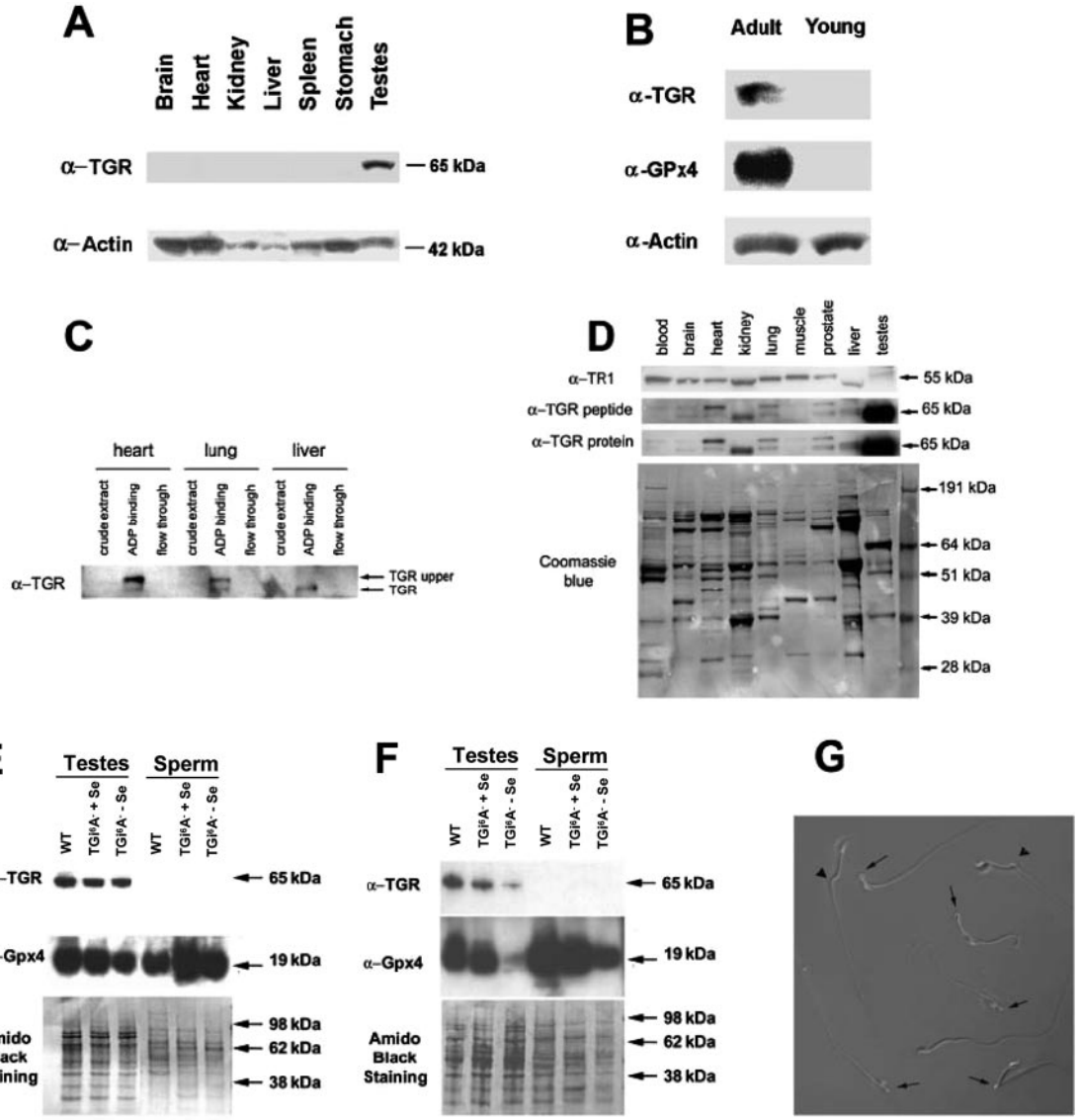

FIG. 2. **Expression pattern of TGR and its regulation by selenium.** *A*, TGR abundance in various mouse tissues. Crude extracts of indicated mouse tissues were separated by SDS-PAGE and analyzed by immunoblot assays with antibodies specific for the C-terminal peptide of TGR (*upper panel*) or actin (*lower panel*). *B*, expression of TGR in adult mouse testes. Crude extracts of mouse testes from 7-month-old (*adult*) and 20-day-old (*young*) mice were separated by SDS-PAGE and analyzed by immunoblot assays with antibodies specific for TGR (*upper panel*), GPx4 (*middle panel*), or actin (*lower panel*). *C*, enrichment of TGR using ADP-Sepharose. Crude extracts from indicated mouse tissues were applied to an ADP-Sepharose column, and bound and unbound fractions were analyzed by immunoblot assays. TGR could be seen in ADP-Sepharose bound fractions as 65- (*TGR*) and/or 70-kDa (*TGR upper*) species. *D*, detection of TGR in mouse tissues. TGR samples were enriched using ADP-Sepharose and detected by immunoblot assays using antibodies specific to TR1 (*top panel*), the C-terminal peptide of TGR (*second panel from top*), or recombinant TGR (*third panel from top*), followed by Coomassie Blue staining (*bottom panel*). *E*, TGR and GPx4 expression in testes and epididymal sperm. Immunoblot analyses of TGR (*upper panel*) and GPx4 (*middle panel*) and protein staining with Amido Black (*lower panel*) in testes and sperm samples from a wild type mouse maintained on the selenium-sufficient diet (*WT*), an i^6A^- mutant Sec $tRNA^{[Ser]Sec}$ mouse maintained on the selenium-sufficient diet for 3 months (*TGi⁶A + Se*), and in a i^6A^- mutant Sec $tRNA^{[Ser]Sec}$ mouse maintained on the selenium-deficient diet for 3 months (*TGi⁶A − Se*) are shown. *F*, prolonged selenium deficiency in transgenic mice. Immunoblot analyses were done as in *E* except that mice were maintained on the diets for 6 months. *G*, epididymal sperm from i^6A^- transgenic mice maintained on the selenium-deficient diet for 6 months. The sperm were characterized by abnormalities associated with the sperm midpiece (shown by *arrows*).

RESULTS

TGR Is Abundant in Testes after Puberty and Expressed at Low Levels in Other Organs—TGR mRNA was previously detected in testes by Northern blot analyses (8). We tested the expression of this protein by immunoblot assays (Fig. 2*A*). TGR was abundant in mouse testes but was not detected in crude extracts of brain, heart, kidney, liver, spleen, or stomach. To test whether TGR expression might be relevant to testis function, we examined its levels in mice at different ages. TGR was not detected in the testes of a 20-day-old mouse, whereas it was highly expressed in 7-month-old mouse testes (Fig. 2*B*). Control experiments with GPx4, a selenoprotein involved in male reproduction (13, 21), also revealed puberty-dependent expression (Fig. 2*B*).

Although these experiments suggested a possible exclusive presence of TGR in postpubertal testes, analyses of the NCBI EST data base revealed a number of human, mouse, and rat TGR ESTs from other organs and tissues, in addition to those from testes that accounted for the majority of TGR ESTs. To test whether TGR was present in other tissues at levels not detectable by Northern and immunoblot assays, we employed ADP-Sepharose affinity chromatography to enrich for possible TGR in each of the analyzed tissue samples. This procedure allows selective enrichment of NADPH-dependent oxidoreductases, including TRs (22). When the enriched fractions were

tested for the presence of TGR by immunoblot assays, the enzyme was detected in heart, lung, and liver samples (Fig. 2*C*). Using this approach, we found TGR in all mouse tissues studied, including liver, kidney, brain, lung, heart, muscle, and prostate (detected as 65- or 70-kDa species on SDS-polyacrylamide gels) (Fig. 2*D*). As expected, TGR levels in the testes were dramatically higher than in any other examined tissues, and this enzyme could be seen as one of the major Coomassie Blue-stained bands in the ADP-Sepharose-enriched testis fraction (Fig. 2*D*). In contrast, TR1 was more uniformly distributed in mouse tissues. The pattern of low abundance of TGR in most tissues and its high expression in testes was reminiscent of that of GPx4 (23).

Effects of Selenium Deficiency and Defects in Sec Biosynthesis on TGR Expression—Because TGR is a selenoprotein, we tested the roles of dietary selenium and a defect in Sec biosynthesis in the regulation of TGR expression. Sec biosynthesis requires a unique $tRNA^{[Ser]Sec}$, a *cis*-acting selenocysteine insertion sequence element, and several *trans*-acting components (24). We previously generated a mouse model of selenoprotein deficiency by overexpressing an i^6A^- mutant Sec $tRNA^{[Ser]Sec}$ that resulted in reduced selenoprotein expression under normal dietary levels of selenium (19). TGR expression in testes appeared to be little affected, even when i^6A^- mice were maintained on the selenium-deficient diet for 3 months, and this pattern was again similar to that of GPx4 (25) (Fig. 2*E*). However, a prolonged selenium-deficiency (6 months) of i^6A^- mice decreased both TGR and GPx4 levels in testes (Fig. 2*F*). Interestingly, sperm from i^6A^- mice that were maintained on the selenium-deficient diet for 6 months had lower motility and a higher proportion of abnormal morphology compared with sperm from control mice (~75 *versus* ~15% abnormal sperm, respectively), and the most common defects were seen in the midpiece region of the selenium-deficient i^6A^- sperm (Fig. 2*G*). These results were consistent with the previously suggested role of selenium in sperm motility and midpiece stability (26).

To determine whether TGR, similarly to GPx4 (13), was maintained after completion of spermiogenesis, we tested the presence of both enzymes in epididymal sperm. Immunoblot assays revealed the lack of TGR in sperm, whereas GPx4 was present in large quantities (Fig. 2, *E* and *F*).

Spermatid Location of TGR—We further employed light (Fig. 3*A*) and confocal (supplemental Fig. S1) microscopy to determine the location of TGR in testes. Spermatids exhibited a strong TGR signal, but the enzyme was also detected in spermatocytes. Consistent with the immunoblot data, no TGR signal was detected in sperm. Control experiments with GPx4 revealed that this enzyme accumulated in spermatids; it was abundant in the midpiece of mature sperm (supplemental Fig. S1) as previously reported (13). Thus, TGR and GPx4 accumulated during spermatid development. However, TGR was lost, and GPx4 remained after the spermatids differentiated into mature sperm. Light and confocal microscopy also revealed that TGR had a broad distribution, including the cytoplasm and nucleus, as previously reported for GPx4 (16, 23, 27).

We next used electron microscopy to determine the specific location of TGR in late spermatids. The enzyme appeared very abundant in the cytoplasm of step 15–17 spermatids, at the time of mitochondrial sheath formation in the sperm tail midpiece. Moreover, in these spermatids TGR accumulated near the site of mitochondrial sheath assembly (Fig. 3*B*).

Disulfide Bond Isomerization by TGR—Parallels in temporal and spatial expression patterns between TGR and GPx4, as well as dependence of these redox enzymes on selenium, suggested that functions of TGR and GPx4 might be linked. To test this hypothesis, we solubilized epididymal sperm and used H_2O_2 to induce oxidative cross-links between GPx4 and sperm

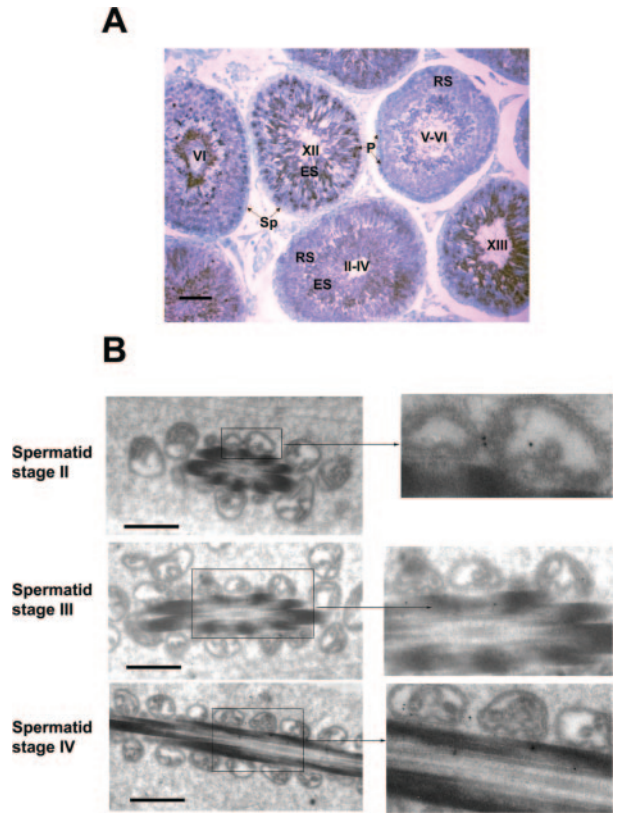

FIG. 3. **Localization of TGR in mouse testes.** *A*, light microscopic localization of TGR revealed by immunoperoxidase staining with anti-TGR antibodies. *RS*, round spermatids; *ES*, elongated spermatids; *P*, pachytene spermatocytes; *Sp*, spermatogonia. There is intense TGR immunostaining in the cytoplasm of elongated spermatids. *Roman numerals* indicate stages of the cycle of the seminiferous epithelium. *Bar*, 50 μm. *B*, immunogold localization of TGR near the midpiece in elongating spermatids. In Step 16 spermatids (*stages II–III*), TGR immunolabeling was seen in the vicinity of the assembling mitochondrial sheath. Labeling was also associated with the periphery of the mitochondria and was occasionally seen within the mitochondria. In Step 17 spermatids (*stage IV*), when mitochondria begin to condense, elongate, and helically wind around the axoneme, TGR labeling was randomly localized throughout the cytoplasm and was still associated with the mitochondrial sheath. *Bar*, 0.5 μm.

proteins (13). GPx4 efficiently participated in oxidative cross-links, migrating as heterogeneous high molecular weight species in non-reducing SDS-polyacrylamide gels (Fig. 4*A*, *upper panel*, *first lane*). However, in reducing SDS-polyacrylamide gels, such cross-links were disrupted and GPx4 migrated as a ~17-kDa monomeric protein (Fig. 4*A*, *lower panel*). Heterogeneous oxidative cross-links could be completely reduced by 5 mM GSH (Fig. 4*A*, *lane 4*). This observation provided an important control but was unlikely to be of physiological significance as GSH levels are extremely low in sperm (26). Purified testis TR1 in the presence of NADPH had no effect on the GPx4 cross-links (Fig. 4*A*, *upper panel*, *lane 2*). However, TGR in the presence of NADPH dramatically affected the cross-linking pattern, generating a ~46-kDa GPx4-containing species in place of the heterogeneous high molecular weight species (Fig. 4*A*, *lane 3*). This effect could not be attributed exclusively to GPx4 reduction by TGR, as no significant monomeric GPx4 was detected. The 46-kDa species also had a different mass than either a possible GPx4 dimer or a GPx4·TGR complex and were formed by TGR in a concentration-dependent manner (Fig. 4*B*). Therefore, these data suggested that TGR promoted isomerization of disulfide bonds formed between GPx4 and certain sperm protein(s), generating a 46-kDa species containing GPx4 from high molecular weight nonspecific cross-links.

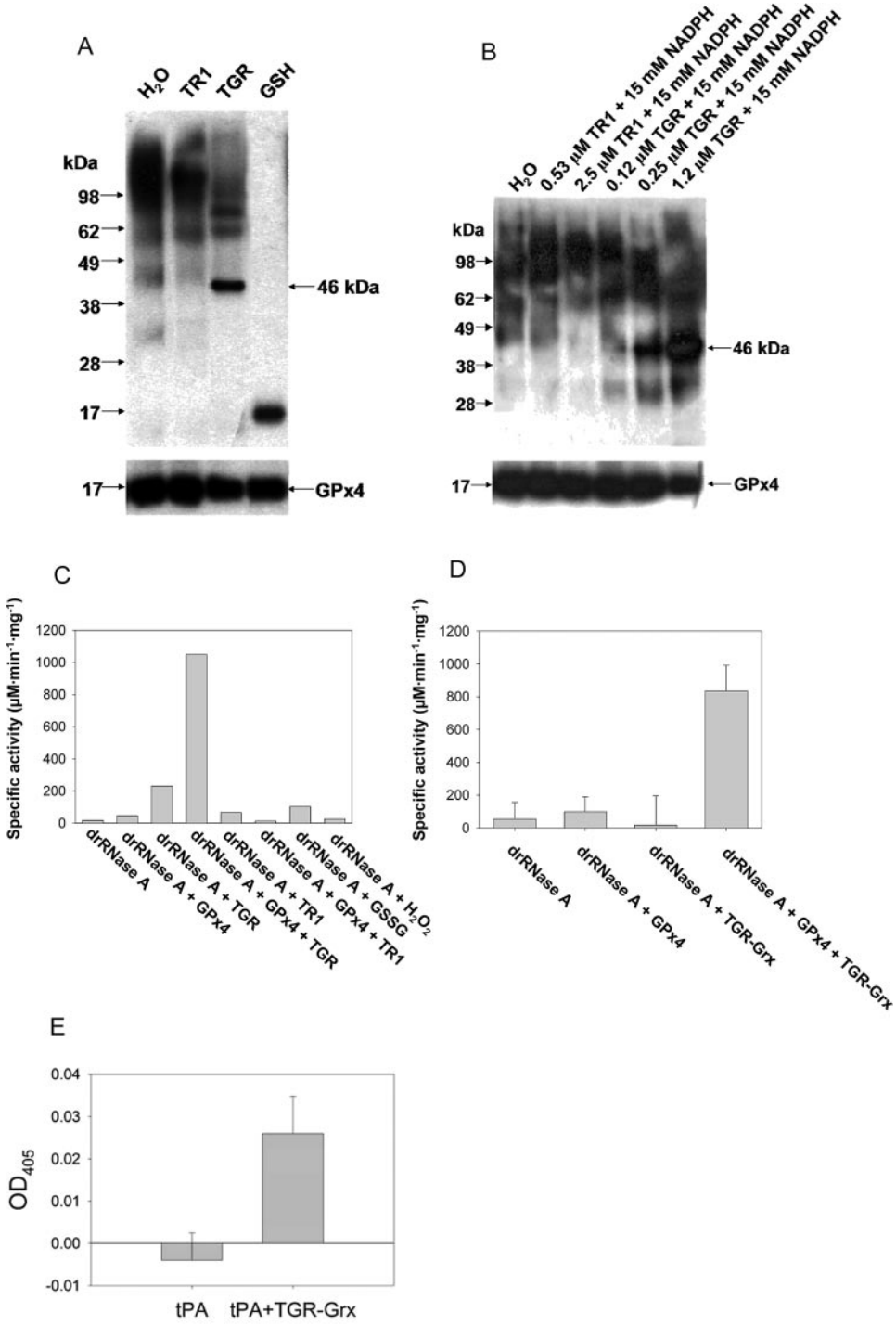

FIG. 4. **Disulfide bond isomerase activity of TGR.** *A*, isomerization of GPx4 cross-links by TGR. Epididymal sperm was solubilized according to Ursini *et al.* (13) and treated with water (used as control, *lane 1*), 2.5 μM purified testis TR1 in the presence of 15 mM NADPH (*lane 2*), 2.5 μM purified testis TGR in the presence of 15 mM NADPH (*lane 3*), or 5 mM GSH (*lane 4*). 80 μM H_2O_2 was then added to each sample, followed by incubation at room temperature for 15 min. The samples were resolved by SDS-PAGE under non-reducing (*upper panel*) and reducing (*lower panel*) conditions, followed by immunoblot assays with anti-GPx4 antibodies. Locations of the GPx4 monomer and the ~46-kDa species are indicated on the right and migration of protein standards on the left of the gels. *B*, concentration dependence of isomerization of GPx4 cross-links by TGR. This experiment was performed as in *A*, except that the samples were treated with indicated concentrations of TR1 and TGR. *C*, isomerization of disulfide bonds in RNase A by TGR. 5 mM cCMP was incubated with 1 μM denatured and reduced RNase A in 0.5 ml of PBS, pH 7.4, for 45–60 min. RNase A activity is shown, which was determined by following the hydrolysis of cCMP as an increase in absorbance at 296 nm ($\Delta\epsilon_{296} = 0.19\ mM^{-1}\cdot cm^{-1}$). These experiments were performed in the presence of 2 μM H_2O_2-oxidized *L. esculentum* GPx4, as isolated 1 μM TGR, 1 μM TR1, or combinations of GPx4 with either TGR or TR1 as described under "Experimental Procedures." In control experiments, 2 μM oxidized glutathione or 2 μM H_2O_2 were used as alternative oxidants. *D*, disulfide bond isomerase activity of TGR is located in its Grx domain. This set of experiments was performed as in *C*, except that 7 μM recombinant Grx domain of TGR was used. *E*, Grx domain of TGR stimulates activity of an *E. coli*-expressed tPA. The periplasmic fractions of wild type cells expressing periplasmic tPA, and wild type cells expressing both tPA and the Grx domain of TGR in the periplasm were subjected to plasminogen activation assays (tPA activity as expressed a change in absorbance at 405 nm) as described under "Experimental Procedures." The periplasmic fractions of wild type cells and wild type cells expressing the Grx domain alone were used as controls, and their background tPA activities were not significantly different from that of wild type cells expressing tPA alone. S.D. is shown as *error bars* based upon four independent measurements.

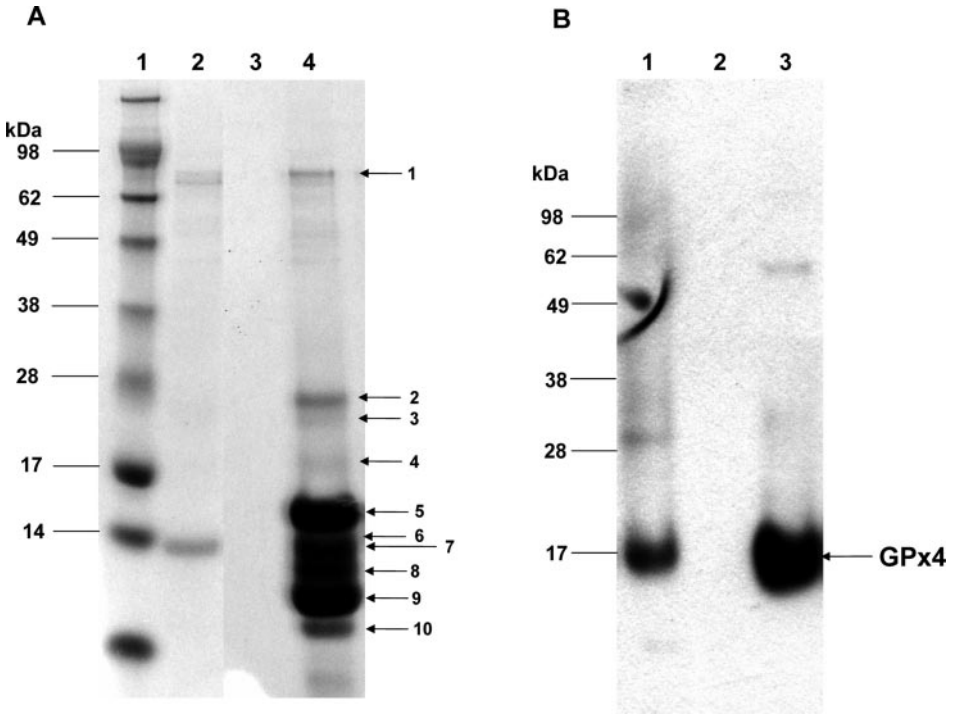

FIG. 5. **TGR targets in rat sperm.** *A*, identification of TGR targets in rat sperm. The purified recombinant TGR Grx domain was immobilized on a column and used as bait to bind target proteins in solubilized sperm as described under "Experimental Procedures." The targets were eluted with DTT and visualized by Coomassie Blue staining on an SDS-polyacrylamide gel. *Lane 1*, protein standards; *lane 2*, solubilized sperm; *lane 3*, DTT-eluted fraction from a control column that lacked the Grx domain; *lane 4*, DTT-eluted fraction from the Grx domain column. The proteins indicated by the *numbers* were identified and are listed in Table I. The lower bands represent the Grx domain. *B*, GPx4 is a TGR target. Protein fractions shown in *A* were subjected to a Western blot analysis with antibodies against GPx4. *Lane 1*, solubilized sperm; *lane 2*, DTT-eluted fraction from a control column; *lane 3*, DTT-eluted fraction from a Grx domain affinity column. The location of GPx4 band is indicated.

TABLE I
TGR targets in rat sperm

Proteins were enriched using the Grx domain affinity column as shown in Fig. 5*A*, and their identities were determined by mass spectrometry and shown in the table.

Protein band	Band size	Protein size	Protein ID
	kDa	*kDa*	
1	~80	74.1	Outer dense fiber of sperm tails 2 (ODF2)
2	~26	27	Glutathione *S*-transferase M5 (GSTM5)
	~26	20.9	Phosphatidylethanolamine-binding protein
3	~24	29.6	Outer dense fiber protein (ODF1)
	~24	17.1	Mitochondrial capsule selenoprotein
4	17	20	Phospholipid hydroperoxide glutathione peroxidase (GPx4)
6	14	15.3	Testis lipid-binding protein
	14	16	Hemoglobin β chain
5 and 7–10			Mouse TGR Grx domain (bait protein)

GPx4 was reported to be involved in disulfide bond formation in sperm proteins (13, 26), and its homologs and other thiol peroxidases were implicated in regulating cellular processes by H_2O_2-dependent disulfide bond formation. For example, yeast GPx4 homolog, Hyr1/Gpx3, formed a specific disulfide bond in transcription factor Yap1 in response to H_2O_2 treatment in *Saccharomyces cerevisiae* (28). However, for generation of correct disulfide bonds, both disulfide bond formation and isomerization processes are necessary, and the latter process is dependent on availability of an electron donor. GPx4 is unlikely to isomerize disulfide bonds because of its peroxidase function. In contrast, NADPH-dependent TGR would fit the disulfide bond isomerase function.

We directly tested whether TGR had disulfide bond isomerization activity by using denatured reduced RNase A as substrate and a recombinant H_2O_2-oxidized *L. esculentum* GPx4 homolog as a thiol oxidant. When used separately, GPx4 and TGR had little effect on RNase A activation (Fig. 4*C*). However, the use of both of these enzymes resulted in RNase A activity, demonstrating that TGR indeed catalyzes disulfide bond isomerization (Fig. 4*C*). In contrast, TR1 alone, TR1 in combination with GPx4, oxidized glutathione, or H_2O_2 did not generate functional RNase A. The Grx domain of TGR in combination with GPx4 could also isomerize disulfide bonds in RNase A (Fig. 4*D*), suggesting that this domain directly attacked disulfides generated by GPx4 in RNase A and that it was responsible for the disulfide reshuffling activity of TGR.

To test whether TGR could promote disulfide bond isomerization in an *in vivo* system, we expressed the Grx domain of TGR in *E. coli* and targeted it to the periplasm by using a signal peptide. To assay disulfide bond isomerization, we expressed human tPA, which has 17 disulfide bonds, in *E. coli* periplasm. Co-expression of tPA and an *E. coli* disulfide bond isomerase DsbC is known to increase tPA activity (29). Targeting mammalian protein disulfide isomerase to the *E. coli* periplasm also can partially stimulate tPA activity. We found that when co-

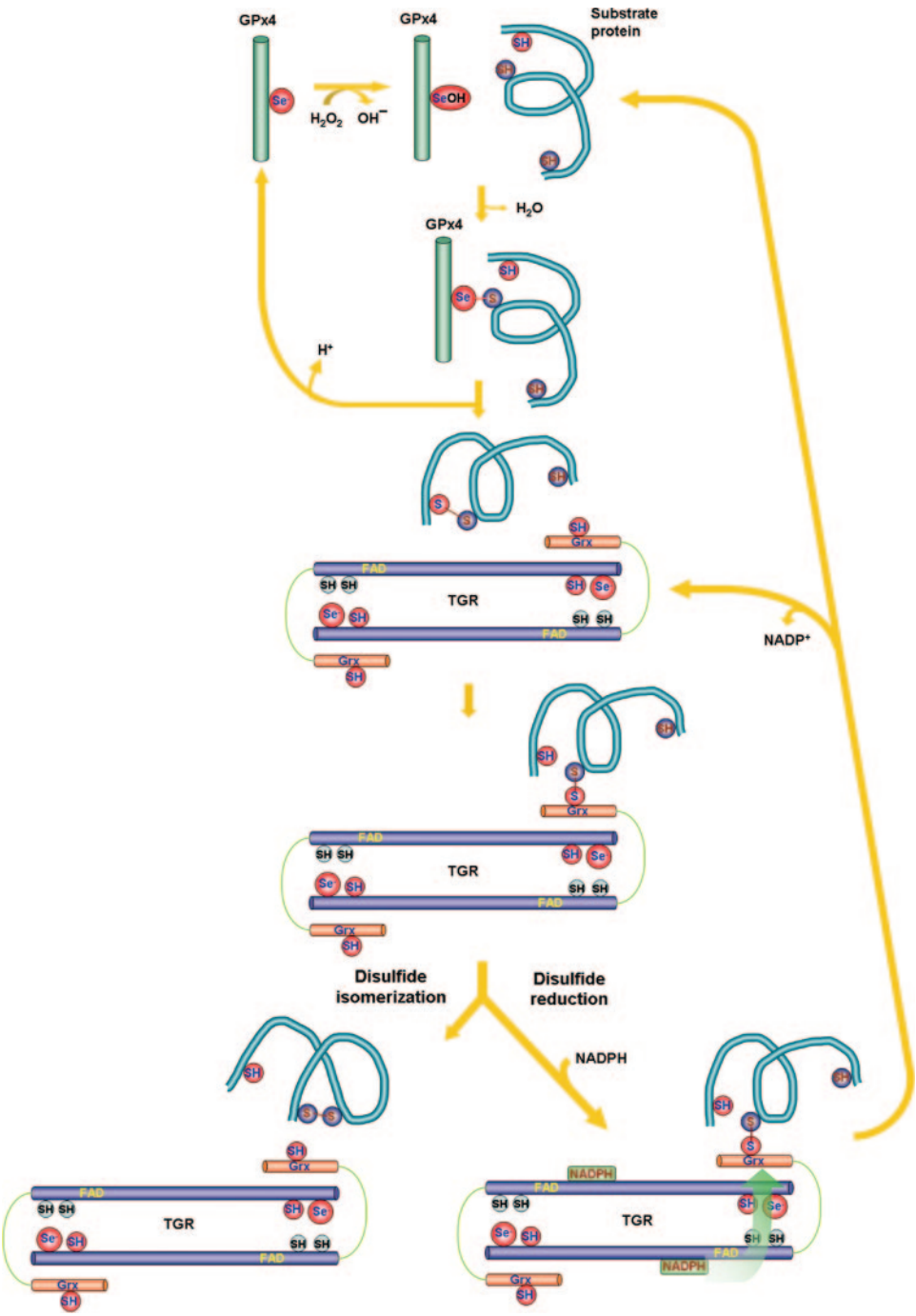

FIG. 6. **A model for disulfide bond formation by TGR.** The proposed mechanism of disulfide bond formation in substrate proteins involves thiol peroxidase GPx4 and disulfide isomerase/reductase TGR. GPx4 is initially oxidized to selenenic acid by H_2O_2 (or other peroxides), followed by reduction of the selenenic acid by a substrate protein, generating a disulfide bond in this protein. If the disulfide bond is formed incorrectly, TGR attacks it by the catalytic thiol located in the Grx domain to form a mixed Grx (*TGR*) substrate-protein disulfide. This intermolecular disulfide can either collapse into a correct disulfide bond in the substrate protein and a reduced Grx domain (isomerase function), or result in reduction of a non-productive intermolecular disulfide bond (reductase function). The latter is accomplished by the NADPH-dependent reduction of the C-terminal penultimate selenocysteine center (via FAD and a thiol/disulfide active site), followed by the attack by the selenolate on the intermolecular disulfide. Because GPx4 is itself a substrate for disulfide bond isomerization by TGR, this system could also reshuffle disulfide bonds between GPx4 and other substrate proteins.

expressed with the Grx domain of TGR, tPA had higher activity compared with cells expressing tPA only, consistent with the disulfide isomerase activity of the Grx domain (Fig. 4*E*).

We further reasoned that in the absence of the natural electron donor (the TR portion of TGR), the mixed disulfides formed between the Grx domain and natural substrates would be stable. We explored this idea by using the Grx domain as a bait to trap and identify natural TGR targets. We prepared an affinity column containing the Grx domain and used it to bind proteins from a solubilized rat sperm extract. After extensive washing, the proteins were eluted with DTT, visualized by SDS-PAGE (Fig. 5*A*), and identified by mass spectrometry sequencing (Table I). Eight proteins were identified by this procedure. Interestingly, among these, mitochondrial capsule selenoprotein (30), two outer dense fiber proteins (31, 32), and glutathione *S*-transferase M5 (33) are known as structural components of the midpiece and tail regions of sperm, and expression of all identified target proteins except one (hemo-

globin) dramatically increases in elongating spermatids. Consistent with our findings that GPx4 is a substrate of TGR, this enzyme was among the proteins trapped by the Grx affinity column (Fig. 5, *A* and *B* and Table I).

DISCUSSION

Selenium has long been known to be necessary for male reproduction. Initial studies suggested that a mitochondrial capsule selenoprotein mediated this effect, whereas recent studies revealed that this effect is because of the antioxidant and structural functions of GPx4 (13, 34). Our study now indicates a role for an additional selenoprotein, TGR, in sperm maturation. We propose that this protein may isomerize disulfide bonds in spermatids thus promoting formation of structural components of sperm.

Formation of disulfide bonds in proteins is a catalytic process that involves multiple designated redox proteins. Known pathways for disulfide bond formation operate in the endoplasmic reticulum of eukaryotic cells and bacterial periplasm (35), and an additional viral pathway has been described in infected mammalian cells (36). These pathways are similarly organized. In particular, in each pathway, the formation and isomerization of disulfide bonds in substrate proteins is catalyzed by a thiol/disulfide oxidoreductase that exhibits thioredoxin fold and possesses a catalytic C*xx*C motif. The disulfide bonds in thiol/disulfide oxidoreductases are further donated to adaptor redox proteins, which are often membrane-bound, and finally to an electron transport chain or directly to molecular oxygen (35).

The periplasmic and endoplasmic reticulum pathways of disulfide bond formation and isomerization, however, do not explain how disulfide bonds are formed in many other locations in cells and tissues. For example, in testes, the process of sperm development and maturation is dependent upon the formation of disulfide bonds in structural proteins. Our findings suggested a role of TGR in this process as a disulfide isomerase. The experiments also established that TGR and GPx4 may constitute a novel disulfide bond formation and isomerization system that operates during spermiogenesis.

During later stages of spermiogenesis, mitochondria attach to outer dense fiber proteins of axoneme in the sperm midpiece region, and the structure is stabilized by numerous disulfide bonds in various proteins. Thereafter, the spermatid cytoplasm shrinks, and the plasma membrane is attached to the midpiece of the sperm. Two plasma membrane proteins, phosphatidylethanolamine-binding protein and lipid-binding protein, which are highly expressed in late spermatids, were found as TGR targets, suggesting that these proteins might also be involved in disulfide-linked sperm structures. Overall, our data suggested that the disulfide bond formation system involving GPx4 and TGR may play an important role in arranging a complex network of spermatid proteins via structural disulfide bonds.

Our current view on the mechanism of disulfide bond formation and isomerization in substrate sperm proteins, which involves thiol peroxidase GPx4 and disulfide bond isomerase TGR, is shown in Fig. 6. This novel disulfide forming system is principally different from those operating in either eukaryotic ER (37) or bacterial periplasm (38), which employ C*xx*C motif-containing thiol/disulfide oxidoreductases for both disulfide bond formation and isomerization and oxygen or electron transport chain as electron acceptors (39). Substrate specificity of the GPx4/TGR system also suggests a source of electron acceptors for disulfide bond formation (*i.e.* H_2O_2 or other hydroperoxides) and electron donors for disulfide bond isomerization/reduction (*i.e.* NADPH) in testes. Moreover, the presence of TGR and GPx4 in various tissues and cellular compartments points to possible roles of these proteins in disulfide bond formation, which are not limited to mitochondrial sheath assembly.

Acknowledgments—We thank Gautam Sarath and Ronald Cerny for proteomic analyses, and Paul Copeland, Donna Driscoll, Han Asard, Martin Dickman, Jonathan Beckwith, and George Georgiou for providing antibodies, strains, or constructs. The use of ^{75}Se is supported by DoE DE-FG07-02ID14380.

REFERENCES

1. Holmgren, A. (1980) *Experientia Suppl.* **36,** 149–180
2. Gladyshev, V. N., Jeang, K. T., and Stadtman, T. C. (1996) *Proc. Natl. Acad. Sci. U. S. A.* **93,** 6146–6151
3. Tamura, T., and Stadtman, T. C. (1996) *Proc. Natl. Acad. Sci. U. S. A.* **93,** 1006–1011
4. Arnér, E. S., and Holmgren, A. (2000) *Eur. J. Biochem.* **267,** 6102–6109
5. Nalvarte, I., Damdimopoulos, A. E., Nystom, C., Nordman, T., Miranda-Vizuete, A., Olsson, J. M., Eriksson, L., Bjornstedt, M., Arnér, E. S., and Spyrou, G. (2004) *J. Biol. Chem.* **279,** 54510–54517
6. Jakupoglu, C., Przemeck, G. K., Schneider, M., Moreno, S. G., Mayr, N., Hatzopoulos, A. K., de Angelis, M. H., Wurst, W., Bornkamm, G. W., Brielmeier, M., and Conrad, M. (2005) *Mol. Cell. Biol.* **25,** 1980–1988
7. Conrad, M., Jakupoglu, C., Moreno, S. G., Lippl, S., Banjac, A., Schneider, M., Beck, H., Hatzopoulos, A. K., Just, U., Sinowatz, F., Schmahl, W., Chien, K. R., Wurst, W., Bornkamm, G. W., and Brielmeier, M. (2004) *Mol. Cell. Biol.* **24,** 9414–9423
8. Sun, Q. A., Wu, Y., Zappacosta, F., Jeang, K. T., Lee, B. J., Hatfield, D. L., and Gladyshev, V. N. (1999) *J. Biol. Chem.* **274,** 24522–24530
9. Sun, Q. A., Kirnarsky, L., Sherman, S., and Gladyshev, V. N. (2001) *Proc. Natl. Acad. Sci. U. S. A.* **98,** 3673–3678
10. Rundlöf, A. K., Janard, M., Miranda-Vizuete, A., and Arnér, E. S. (2004) *Free Radic. Biol. Med.* **36,** 641–656
11. Su, D., and Gladyshev, V. N. (2004) *Biochemistry* **43,** 12177–12188
12. Ursini, F., Maiorino, M., and Roveri, A. (1997) *Biomed. Environ. Sci.* **10,** 327–332
13. Ursini, F., Heim, S., Kiess, M., Maiorino, M., Roveri, A., Wissing, J., and Flohe, L. (1999) *Science* **285,** 1393–1396
14. Sadek, C. M., Damdimopoulos, A. E., Pelto-Huikko, M., Gustafsson, J. A., Spyrou, G., and Miranda-Vizuete, A. (2001) *Genes Cells* **6,** 1077–1090
15. Miranda-Vizuete, A., Ljung, J., Damdimopoulos, A. E., Gustafsson, J. A., Oko, R., Pelto-Huikko, M., and Spyrou, G. (2001) *J. Biol. Chem.* **276,** 31567–31574
16. Pfeifer, H., Conrad, M., Roethlein, D., Kyriakopoulos, A., Brielmeier, M., Bornkamm, G. W., and Behne, D. (2001) *FASEB J.* **15,** 1236–1238
17. Sutovsky, P., Tengowski, M. W., Navara, C. S., Zoran, S. S., and Schatten, G. (1997) *Mol. Reprod. Dev.* **47,** 79–86
18. Sun, Q. A., and Gladyshev, V. N. (2002) *Methods Enzymol.* **347,** 451–461
19. Moustafa, M. E., Carlson, B. A., El-Saadani, M. A., Kryukov, G. V., Sun, Q. A., Harney, J. W., Hill, K. E., Combs, G. F., Feigenbaum, L., Mansur, D. B., Burk, R. F., Berry, M. J., Diamond, A. M., Lee, B. J., Gladyshev, V. N., and Hatfield, D. L. (2001) *Mol. Cell. Biol.* **21,** 3840–3852
20. Bessette, P. H., Aslund, F., Beckwith, J., and Georgiou, G. (1999) *Proc. Natl. Acad. Sci. U. S. A.* **96,** 13703–13708
21. Foresta, C., Flohe, L., Garolla, A., Roveri, A., Ursini, F., and Maiorino, M. (2002) *Biol. Reprod.* **67,** 967–971
22. Sun, Q. A., Zappacosta, F., Factor, V. M., Wirth, P. J., Hatfield, D. L., and Gladyshev, V. N. (2001) *J. Biol. Chem.* **276,** 3106–3114
23. Roveri, A., Casasco, A., Maiorino, M., Dalan, P., Calligaro, A., and Ursini, F. (1992) *J. Biol. Chem.* **267,** 6142–6146
24. Hatfield, D. L., and Gladyshev, V. N. (2002) *Mol. Cell. Biol.* **22,** 3565–3576
25. Lei, X. G., Ross, D. A., Parks, J. E., and Combs, G. F., Jr. (1997) *Biol. Trace Elem. Res.* **59,** 195–206
26. Maiorino, M., and Ursini, F. (2002) *Biol. Chem.* **383,** 591–597
27. Borchert, A., Savaskan, N. E., and Kuhn, H. (2003) *J. Biol. Chem.* **278,** 2571–2580
28. Delaunay, A., Pflieger, D., Barrault, M. B., Vinh, J., and Toledano, M. B. (2002) *Cell* **111,** 471–481
29. Qiu, J., Swartz, J. R., and Georgiou, G. (1998) *Appl. Environ. Microbiol.* **64,** 4891–4896
30. Nam, S. Y., Maeda, S., Ogawa, K., Kurohmaru, M., and Hayashi, Y. (1997) *J. Vet. Med. Sci.* **59,** 983–988
31. Burmester, S., and Hoyer-Fender, S. (1996) *Mol. Reprod. Dev.* **45,** 10–20
32. Morales, C. R., Oko, R., and Clermont, Y. (1994) *Mol. Reprod. Dev.* **37,** 229–240
33. Fulcher, K. D., Mori, C., Welch, J. E., O'Brien, D. A., Klapper, D. G., and Eddy, E. M. (1995) *Biol. Reprod.* **52,** 41–49
34. Strauss, E. (1999) *Science* **285,** 1339
35. Sevier, C. S., and Kaiser, C. A. (2002) *Nat. Rev. Mol. Cell. Biol.* **3,** 836–847
36. Senkevich, T. G., White, C. L., Koonin, E. V., and Moss, B. (2002) *Proc. Natl. Acad. Sci. U. S. A.* **99,** 6667–6672
37. Fassio, A., and Sitia, R. (2002) *Histochem. Cell Biol.* **117,** 151–157
38. Kadokura, H., Katzen, F., and Beckwith, J. (2003) *Annu. Rev. Biochem.* **72,** 111–135
39. Bardwell, J. C. (2002) *Dev. Cell* **3,** 758–760

Su et al.
Supplementary Figure

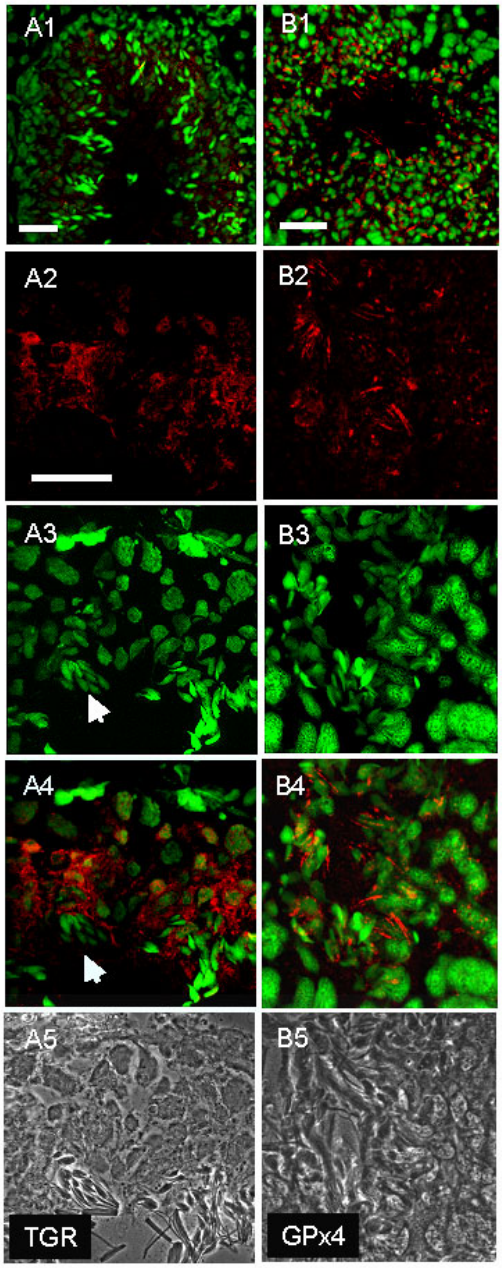

Figure S1. Spermatid Location of TGR in Mouse Testes.
TGR (A1) and GPx4 (B1), shown in red fluorescence, were localized to seminiferous tubules by staining with specific antibodies. TGR pre-immune serum and secondary antibodies alone showed no signal (data not shown). TGR could be seen in the layers consisting of spermatids (A2-A5), but not in mature sperm (shown by arrows in A3-A4), as determined by stained nuclei (green fluorescence) (A1-A4) and phase contrast images (A5). In contrast, GPx4 was detectable in all stages of spermatogenesis with highest levels in the midpieces of the tails of mature spermatozoa (B1-B5). Scale bars: 20 μm (A1 and B1) and 25 μm (A2-A5 and B2-B5).